Journal of Catalysis **197,** 123–130 (2001)
doi:10.1006/jcat.2000.3074, available online at http://www.idealibrary.com on IDEAL®

Selective Catalytic Reduction of NO by Methane over CeO_2–Zeolite Catalysts—Active Sites and Reaction Steps

T. Liese, E. Löffler, and W. Grünert[1]

Lehrstuhl für Technische Chemie, Ruhr-Universität Bochum, D-44 780 Bochum, Germany

Received June 2, 2000; revised September 18, 2000; accepted September 26, 2000

The selective catalytic reduction of NO with methane over catalysts consisting of CeO_2 and H-zeolites (physical mixtures or precipitates of the oxide onto the external surface of the zeolite) has been studied with the aim to establish the catalytic functions required and the basic features of the reaction mechanism. Methods employed include catalytic studies over various catalyst arrangements, e.g., experiments involving the SCR of NO_2 or NO over the catalyst or its individual components (CeO_2, zeolite), and over layered arrangements of these components (typically 1000 ppm NO (NO_2), 1000 ppm CH_4, 2% O_2 in He, 10,000 h^{-1}), studies of NO oxidation activity of catalyst components, and IR spectroscopy in the diffuse reflectance mode. It was found that the NO reduction includes a bifunctional interaction between redox sites at the CeO_2 surface and zeolite Brønsted sites. The oxidation of NO to NO_2, which is part of the reaction mechanism over these catalysts, takes place over the CeO_2 surface, but it is not the only function of CeO_2 in the reaction path that provides an extra activity of the mixed catalysts (as compared to the known activity of H-ZSM-5). From experiments with layered catalyst arrangements, it was concluded that the bifunctional interaction is not mediated by a long-distance transport step as would be gas-phase transport of NO_2. The experimental evidence suggests that methane is activated on the CeO_2 surface, possibly assisted by adsorbed NO_2, and reacts with the latter to form a short-lived intermediate (nitromethane or nitrosomethane), which is detached from the surface. Upon further contact with a CeO_2 surface, this intermediate becomes totally oxidized, releasing the nitrogen in oxidized form. Upon desorption into the zeolite it may be activated by Brønsted sites and undergo reactions resulting in the formation of N_2, carbon oxides, and water.

Key Words: **SCR of NO; methane; zeolites; cerium oxide; bifunctional catalysts.**

INTRODUCTION

Over the past decade, research on the selective catalytic reduction of nitrogen oxides with hydrocarbons (HC-SCR) was mainly driven by the interest to establish a purification technology for net oxidizing exhaust gases from mobile sources (diesel, lean-burn engines) (1–3). This approach is also potentially attractive for stationary sources where the reductant ammonia used today might be replaced by natural gas. So far, the most active catalysts for HC-SCR have been found to exhibit insufficient durability in realistic flue gas mixtures. The attempt to use the methane reductant has been additionally hampered by the relative inertness of the latter, which provides lower activity than other reductants over most catalytic systems (1, 4–7).

We have recently reported a catalytic system composed of CeO_2 and acidic zeolites (precipitate of oxide onto zeolite crystallites or physical mixtures), which provides promising activities with the reductant methane while it performs poorly with propene (8). Experiments with physical mixtures (including subsequent separation and separate study of the components) implied a bifunctional nature of this system: both the CeO_2 and the zeolite catalyze different steps in the reaction mechanism that has to include a transport step between these catalyst components. It has been briefly indicated in (8) that one step catalyzed by the CeO_2 particles is the NO oxidation, that the zeolite acts via its protons, and that the interaction distance between CeO_2 and the zeolite sites is short. In the present paper, the factual basis for this view will be fully described and the implications for the reaction mechanism supported by this system and consequences for related systems will be discussed.

EXPERIMENTAL

CeO_2–zeolite catalyts were prepared as described in (8), but with a variety of zeolites, which were kindly provided by Südchemie, München; Tricat, Bitterfeld; Chemiewerk Bad Köstritz; Alsi Penta, Schwandorf (all Germany), and Elf Aquitaine (France). Several different ZSM-5 materials with Si/Al = 12.5–25 were employed, which will be denoted by Greek letters (α–η). The bulk Si/Al ratios of these materials and a crystallinity parameter derived from their lattice IR spectra ((9), intensity ratio of vibrations at 550 cm^{-1} (five-ring mode) and 450 cm^{-1} (TO_4 deformation mode)) are given in Table 1. For a well-crystalline ZSM-5 this ratio

[1] To whom correspondence should be addressed. Fax: +49 234 3214 115. E-mail: w.gruenert@techem.ruhr-uni-bochum.de.

0021-9517/01 $35.00

TABLE 1

ZSM-5 Zeolite Materials Used in the Preparation of CeO_2/ZSM-5 Catalysts

ZSM-5	α	β	γ	δ	ε	ζ	η
Si/Al (by ICP-AES)	14	19	14	14	12.5	25	25
I (550 cm^{-1})/I (450 cm^{-1})[a]	0.80	0.75	n.d.	0.78	0.82	0.77	0.77

[a] Ratio of lattice vibrations, crystallinity parameter (9), see text; error margin, ±0.02.

is expected to be ≈0.8, which is indeed the case with the materials used.

Cerium hydroxide was precipitated onto the external surface of the zeolites (mostly ZSM-5 in the H form, sometimes NH_4 or Na forms, but also H-BEA, H-MOR, H-Y) by rapidly adding aqueous NH_3 (25%) to a slurry of the zeolite in a cerium nitrate solution. The Ce content was typically 8.2 wt%. Physical mixtures (17.5 wt% Ce) were prepared by mixing CeO_2 (from the calcination of $Ce(NO_3)_3$) with the zeolite after compacting, crushing, and sieving the two components into different mesh fractions (CeO_2, 100–160 μm; zeolite, 250–355 μm). Results obtained by mixing the primary zeolite and CeO_2 particles did not differ significantly from those described below. In some experiments the components were not mixed but applied in consecutive layers. Ce-exchanged ZSM-5 was obtained by exchanging NH_4-ZSM-5(α) with a cerium(III) nitrate solution as described previously (8). The Ce content of this sample was 0.57 wt%, which indicates a theoretical exchange degree of ≈20%. An XPS analysis did not reveal significant Ce enrichment at the external crystallite surfaces while it did with the precipitates (10).

IR spectra (diffuse reflectance mode) were measured with a Nicolet Protegé 460 FTIR spectrometer. The samples were outgassed for 3–4 h in flowing Ar at 773 K prior to data acquisition. IR spectra of adsorbed pyridine were obtained with a Unicam RS1 spectrometer. Pyridine was adsorbed at 423 K, and spectra were recorded after desorption of loosely bound adsorbates at 623 K. During all measurements, the sample temperature was held at 423 K. ^{1}H-MAS NMR spectra were measured with a Bruker MLS 500 spectrometer after previous out-gassing in vacuum at 673 K. ^{27}Al-MAS NMR spectra were recorded with a Bruker ASX 400 instrument. Concentrations of protons and octahedrally coordinated Al nuclei (cf. Fig. 2) were obtained by comparing the areas of the corresponding signals with those of reference samples with known proton or Al concentrations.

The selective catalytic reduction (SCR) of NO with methane was studied in a catalytic microflow reactor feeding 1000 ppm NO, 1000 ppm CH_4, and 2% O_2 in He over 0.8–0.9 g of catalyst at 220 ml min^{-1}. The amount of catalyst was selected to ensure a constant GHSV of 10,000 h^{-1} ("standard reaction conditions"). Prior to each run, the samples were calcined in flowing He at 873 K for 2 h. The products were analyzed by a combination of gas chromatography (O_2, N_2, CH_4), calibrated mass spectrometry (NO, CH_4), and calibrated nondispersive IR photometry (CO, CO_2, N_2O). Test experiments with IR photometric analysis of NO and NO_2 indicated that the latter was not formed in significant amounts under our reaction conditions (11). C and N balances of 100 ± 5% were routinely obtained in the product analyses.

The NO oxidation activity of the catalyst components was studied between 773 and 673 K, feeding 1000 ppm NO and 10% O_2 in He at a space velocity which was 5 times that employed for the investigation of the SCR reaction. For the zeolites (≈93 vol% in physical mixtures), this means a GHSV of ≈55,000 h^{-1}; for CeO_2 (≈7 vol%) the GHSV was ≈700,000 h^{-1} since the standard GHSV in SCR runs (10,000 h^{-1}) corresponds to ≈140,000 h^{-1} relative to the CeO_2 component. The results will be reported in terms of the NO conversion given as the ratio between NO_2 formed and the sum of NO_2 and NO. In the NO oxidation experiment, NO and NO_2 were analyzed by calibrated nondispersive IR photometry.

RESULTS AND DISCUSSION

Selective Reduction of NO with Methane over CeO_2/H-ZSM-5 Catalysts

Figure 1 shows an example for the performance of a CeO_2/H-ZSM-5 precipitate (parent zeolite-β) in the

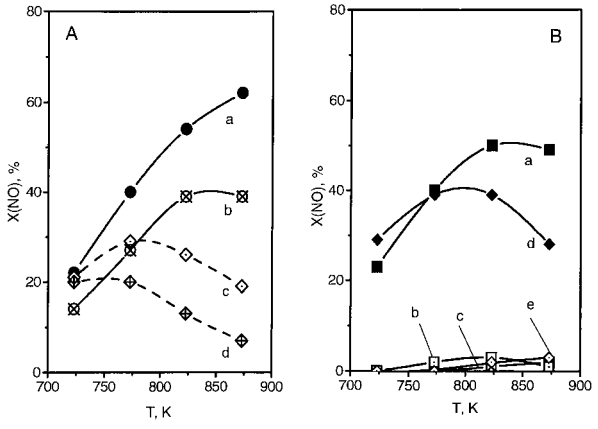

FIG. 1. NO conversions in the selective catalytic reduction of NO by methane over CeO_2/H-ZSM-5 catalysts. GHSV, 10,000 h^{-1}; 1000 ppm NO; 1000 ppm CH_4; and 2% O_2 in He. (A) Precipitates and physical mixtures. Curves: (a) CeO_2/H-ZSM-5(β), by precipitation; (b) CeO_2/H-ZSM-5(β) physical mixture; (c) CeO_2/H-ZSM-5(α) physical mixture; (d) CeO_2/Ce,H-ZSM-5(α) physical mixture. (B) Influence of re-exchange with Na^+ ($NaNO_3$ solution). Curves: (a) CeO_2/Na,H-ZSM-5(δ), by precipitation onto Na-ZSM-5(δ); (b) a, re-exchanged with Na^+ without intermediate treatment; (c) a, re-exchanged with Na^+ after 2 h of calcination in air at 873 K; (d) CeO_2/Ce,H-ZSM-5(α), by precipitation; (e) d, re-exchanged with Na^+.

selective reduction of NO by methane (curve a). The NO conversions given were achieved with methane conversions increasing monotonically from 16% (723 K) to 93% (873 K). Similar data were obtained also with other ZSM-5 materials, e.g., α and γ (see Fig. 3) or δ, as reported in (8). NO conversions up to 65% were measured under standard reaction conditions at temperatures between 823 and 873 K. Above 873 K, the NO conversion decreases again (11). This was observed in an experiment with a less active preparation, which has not been included in Fig. 1. Curve b was measured with a physical mixture of CeO_2 with H-ZSM-5(β). It is obvious that the components display a similar behavior whether exposed as a precipitate or as a physical mixture, with somewhat lower conversions over the latter. A mixture of CeO_2 with the Na form of ZSM-5(β) provided NO conversions of only 3%. Thus, while CeO_2/H-ZSM-5 catalysts are less active than some other catalysts known so far for the selective reduction of NO by methane (e.g., Pt–In/ZSM-5 (12), Co-ZSM-5 (13)), they are attractive for an in-depth study of the catalyst function due to their ability to operate in the form of a physical mixture.

Zeolite Sites Participating in the Bifunctional Reaction Mechanism

These results and the data reported in (8) suggest that the zeolite participates in the mechanism via its acidic sites. However, the catalysts system works under conditions in which solid-state ion exchange would be expected to take place. Figure 2 compares ^{1}H NMR spectra of the CeO_2/H-ZSM-5(δ) precipitate catalyst prior to catalysis, i.e., after vacuum dehydration at 673 K, and after a catalytic run at temperatures between 873 and 673 K. The loss of acidic protons indicated by the signal at ≈4.2 ppm is obvious. Also given are concentrations of octahedreally coordinated Al in these samples as obtained in a parallel ^{27}Al NMR study (11) (the spectra, which exhibit the known signals for tetrahedrally and octahedrally coordinated Al, are not reproduced). The loss of Brønsted sites is larger than could be expected from the extent of dealumination detected. Although this result is not entirely conclusive since ^{27}Al NMR may fail to detect certain forms of extraframework Al (14), some transfer of cerium cations to intrazeolite cation positions appears quite likely. Even a small extent of solid-state ion exchange into zeolite layers adjacent to the CeO_2 crystals may, however, suffice to create a situation described by Yokoyama and Misono (15) wherein NO_2 formed over extrazeolite CeO_2 (or MnO_2) crystals was proposed to facilitate HC-SCR of NO (reductant propene) over intrazeolite Ce ions.

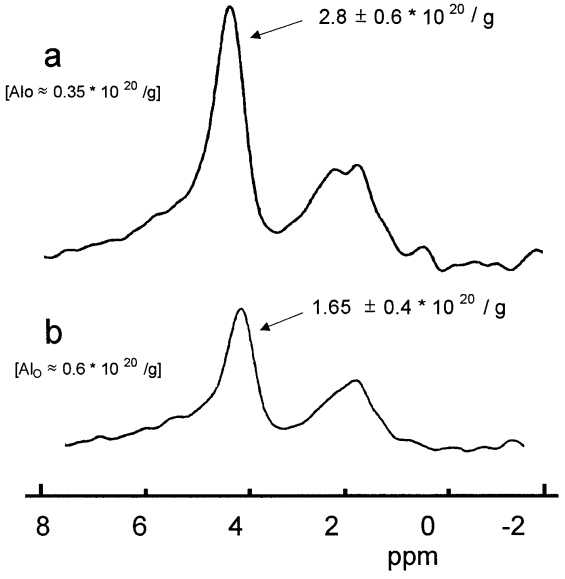

FIG. 2. ^{1}H-MAS NMR spectra of CeO_2/H-ZSM-5(δ), by precipitation. Curves: (a) prior to catalysis (dehydrated by evacuation at 673 K); (b) after catalysis (standard reaction conditions, 873–673 K, for ≈8 h); in brackets, concentrations of octahedrally coordinated Al as evaluated in a parallel ^{27}Al NMR measurement (spectra not shown).

Figure 1 shows further the results of some experiments aiming at the detection of such a possible interaction between extra- and intrazeolite Ce in our system. These experiments were designed to exclude any influence of irreproducibilities, which may occur in the precipitation step of our catalyst preparation. Curves c and d compare the catalytic behavior of physical mixtures of CeO_2 with H-ZSM-5(α) and with the same zeolite partially exchanged with cerium (Ce,H-ZSM-5(α)). This comparison shows that the introduction of Ce ions into ZSM-5 causes the catalytic activity of the mixture to decrease considerably, which is opposite to the observations reported with similar mixtures for the reductant propene (15). With the CH_4 reductant, it is clear that the presence of intrazeolite Ce decreases the activity for selective NO reduction. At the same time it may be noted that there is also a difference between the activities of the physical mixtures of CeO_2 with different H-ZSM-5 materials ((α) and (β), cf. Fig. 1A, curves b and c). This will be discussed below.

Figure 1B reports NO conversions over precipitate catalysts prepared with Na-ZSM-5(δ) or ion-exchanged Ce,H-ZSM-5(α). It is obvious that the NO conversions are quite high even over the preparation with the sodium form (curve a). Since the precipitation was performed with aqueous ammonia, a concomitant partial exchange of Na by NH_4^+ ions, which would result in new acidic sites, may be anticipated: indeed, the residual Na^+ content of this sample as determined by ICP-AES corresponded to an NH_4^+ exchange degree of ≈80%. Part of this material was re-exchanged with Na^+ ions (1 mol/l $NaNO_3$ solution, 298 K, overnight) to poison the acidic protons. This was done in two portions: one of them was re-exchanged without any pretreatment, and the other one was previously calcined in air at 873 K for 2 h in order to stimulate solid-state ion

exchange as is likely to proceed under the reaction conditions. The poisoning of the protons resulted in a total loss of NO reduction activity with or without an intermediate calcination step (Fig. 1B, curves b, c). This implies that the zeolite participates in the reaction mechanism via its protons (or Lewis sites formed from them under reaction conditions), but not via Ce ions that may have been introduced by solid-state ion exchange. The latter was also excluded by the experiment with CeO_2 precipitated on Ce,H-ZSM-5(α). While this preparation still provided a significant activity (curve d), it was completely inactive after the re-exchange treatment with sodium nitrate solution (curve e). It was confirmed by a blank experiment that Ce ions were not removed to any significant extent under the re-exchange conditions employed: the Ce content of the Ce,H-ZSM-5(α) parent zeolite was decreased by only ≈20% by three repeated re-exchange treatments.

The crucial role of zeolite Brønsted sites was strongly supported by a DRIFTS study of catalysts that provided different activities for the selective reduction of NO with methane. Figure 3A summarizes NO conversions obtained under standard reaction conditions over precipitate catalysts prepared with various ZSM-5 parent materials. There are large differences in the performance of the catalysts although no correlation with the bulk Si/Al ratio may be noted: Indeed, the best results were obtained with samples with Si/Al ratios of 14 and 19 while a material with Si/Al ≈ 12.5 is among the inferior catalysts (ε).

No correlation was found between the catalytic activities achieved and various properties of these parent zeolites as crystallinity (cf. Table 1), crystal size, micropore surface area, and external surface area (11). Figures 3B and 3C show IR spectra of the ZSM-5 zeolites used for the preparations (O–H stretching modes, B; combination of O–H stretching and in-plane deformation vibrations, C). In the OH region, the signals at 3610, 3744, 3650, and 3780 cm^{-1} are assigned to zeolite Brønsted sites, silanol groups (external surface or structural defects), and bridging and terminal OH groups of extraframework alumina, respectively (16, 17). It may be noted from Fig. 3B that the zeolites differ strongly with respect to the ratio between the signals for Brønsted sites and silanol groups. This may be partly ascribed to differences in crystal size, but the presence of considerable amounts of extraframework alumina is also obvious in most of the materials studied. ZSM-5 materials providing active catalysts (α, β, γ, cf. Fig. 3A) are characterized by strong bands for Brønsted sites and weak signals for silanol groups. The difference is even more clearly reflected in the region of the combination modes (Fig. 3C), where the silanol combination vibration is expected around 4550 cm^{-1} while the analogous signals of Brønsted sites and bridging OH groups of extraframework alumina should appear at 4660 and 4630 cm^{-1}, respectively (18), and may remain unresolved. In our study, the broad band at 4646 cm^{-1} obviously may be assigned to the combination mode of the Brønsted sites. It is shifted to lower wave numbers in samples in which extraframework aluminium is abundant (e.g., η, ε, α, see Fig. 3B) due to a contribution of the signal from Al–OH groups at lower wave numbers. It may be noted that the signal assigned to Brønsted sites (4646 cm^{-1} or slightly below) is predominant with those parent materials that yield active catalysts.

Since the study of the OH group signals does not exclude a possible role of Lewis sites (extraframework alumina, true

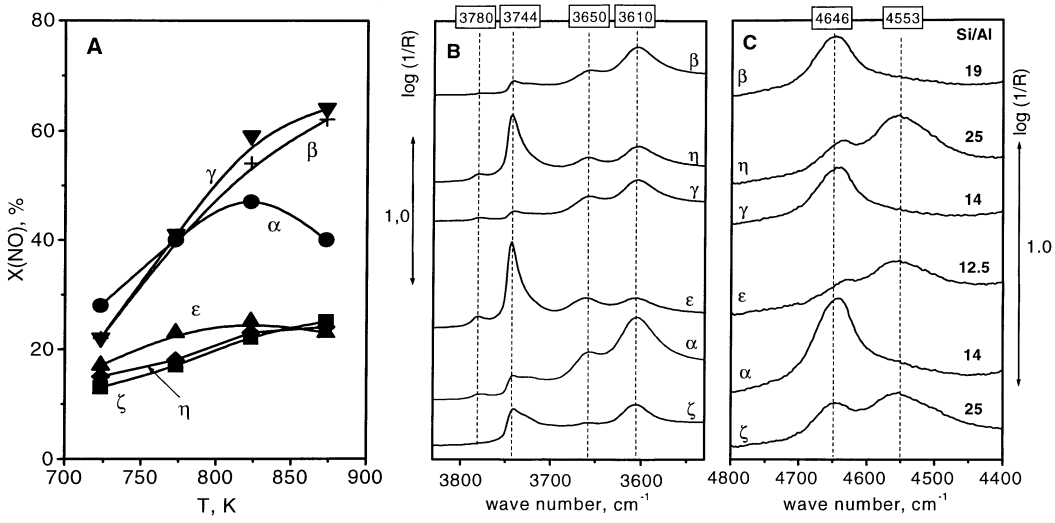

FIG. 3. The role of zeolite protons in the selective catalytic reduction of NO by methane over CeO_2/H-ZSM-5 catalysts. (A) NO conversions over CeO_2/H-ZSM-5 precipitates made of different H-ZSM-5 parent materials (for bulk Si/Al ratio see panel C); GHSV, 10,000 h^{-1}; 1000 ppm NO; 1000 ppm CH_4; and 2% O_2 in He. (B, C) DRIFT spectra of the H-ZSM-5 parent materials: B, OH stretching region; C, region of combination modes between stretching and in-plane deformation vibrations of OH groups.

TABLE 2

Type of Acidity Relevant for the Selective Reduction of NO with Methane over CeO_2/ZSM-5 Catalysts: Intensity Ratios between Signals of Pyridine Adsorbed on Brønsted and Lewis Sites (1540 and 1450 cm^{-1}) of the Parent ZSM-5 Zeolites and NO Conversions over CeO_2/H-ZSM-5 Precipitates Prepared with Them

ZSM-5	α	β	γ	η	ε
I (1540 cm^{-1})/I (1450 cm^{-1})[a]	2,7	3,4	3,7	1,6	0.8
X(NO), %, at 823 K[b]	47	54	59	23	25

[a] Error margin, ±0.3.
[b] Error margin, ±2.

Lewis sites) the role of the latter was investigated by an IR study of pyridine adsorption over the zeolites involved. Table 2 shows intensity ratios between IR bands characteristic of Brønsted and Lewis sites and compares them with NO conversions at 823 K under standard reaction conditions. It is obvious that the highest conversions are obtained with catalysts prepared from materials with high Brønsted/Lewis ratios.

It appears from these results that ZSM-5 materials that are well crystalline as judged from their framework vibrations may exhibit large differences regarding the degree of Al incorporation into the framework. The techniques used to assess this property with low-silica zeolites (^{29}Si and ^{27}Al-MAS NMR) are near their limits of application with the high-silica materials employed here because of the low Al concentration and the fact that some forms of extraframework Al may escape detection by ^{27}Al-MAS NMR (14). The IR approach demonstrated here allowed us to characterize the degree of Al incorporation into the lattice and to conclude that this property, which determines the number of Brønsted sites, is crucial for the activity of CeO_2/H-ZSM-5 catalysts for the selective reduction of NO with methane.

It was also attempted to improve the catalytic activity of a CeO_2/H-ZSM-5 precipitate by increasing the strength of the acidic sites. For this purpose, a ZSM-5 support (α) was subjected to a mild steaming procedure (10% H_2O in He, 800 K), which is known to strongly enhance the hydrocarbon cracking activity (19). The origin of the extra activity is still under debate. A particular acidity of the remaining Brønsted sites due to an interaction with Lewis sites is often inferred (as summarized in (20)), but the effect has been also assigned to an increased Lewis acidity (21). Figure 4A shows the effect of mild steaming on the NO reduction activity of catalysts prepared from the steamed ZSM-5. Figure 4B reports cracking conversions in an *n*-butane cracking experiment, the experimental details of which are given in the legend. While the development of cracking conversions with time-on-stream should not be overemphasized, it is clear that these conversions increase with the length of the *steaming* treatment. With respect to the SCR reaction, however, the same treatment causes a decline of activity (Fig. 4A). Whatever the correct interpretation of the trends in cracking catalysis, this result proves that the zeolite participates in the NO reduction mechanism with its Brønsted sites, and not with its Lewis sites.

NO Oxidation

In the literature, the intermediate oxidation of NO to NO_2 is often assumed to be part of the reaction sequence of HC-SCR (15, 22–27). As to the active site of NO_2 formation, both the redox component (22, 23) and the zeolite protons (or Lewis sites resulting from them) (24–27) have been considered to catalyze the NO oxidation step. We studied the role of a possible NO_2 intermediate over our catalyst system by comparing the reduction of NO and of NO_2 by methane both in the absence and in the presence of oxygen (Fig. 5A, catalysts based on ZSM-5(β)). The results show that the NO reduction is very slow in the absence of oxygen as expected (curve b). NO_2 may be reduced both in the presence and in the absence of oxygen, which supports its role as a reaction intermediate. The lower NO_2 conversion in the *absence* of oxygen (curve d) is due to the high redox activity of CeO_2 (*vide infra*), which leads to a rapid equilibration between NO_2 and NO and, hence, low NO_2 concentrations along the catalyst bed at higher temperatures. The increased NO_2 conversions in the *presence* of 2% oxygen (curve c) may be explained by the higher equilibrium NO_2 concentrations under these conditions.

The property of the CeO_2/zeolite system to operate in the form of physical mixtures allowed us to assess the contribution of both catalyst components to the NO oxidation step individually. For this purpose, the NO oxidation was studied with CeO_2 and various zeolites at a GHSV 5-fold

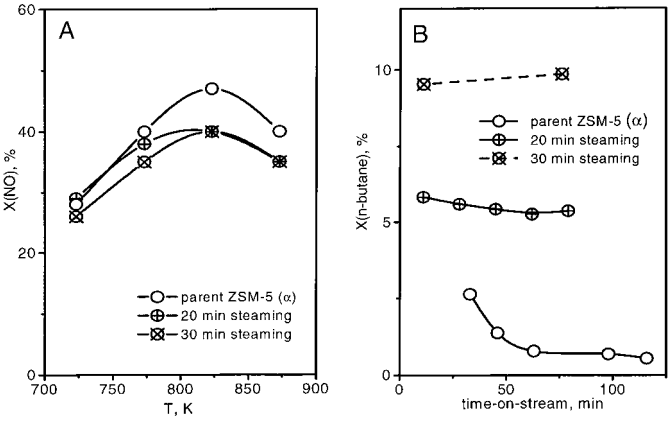

FIG. 4. Performance of mildly steamed ZSM-5(α) in *n*-butane cracking and selective catalytic reduction of NO with methane. Steaming treatment: 10 vol% H_2O in He, 800 K, length as given in the figure. (A) NO conversion in the NO reduction with methane over CeO_2/H-ZSM-5 precipitates prepared from steamed parent zeolite; GHSV, 10,000 h^{-1}; 1000 ppm NO; 1000 ppm CH_4; and 2% O_2 in He. (B) *n*-butane conversion in a cracking experiment over steamed parent zeolite; 50% *n*-butane in Ar; 623 K; GHSV, 2400 h^{-1}.

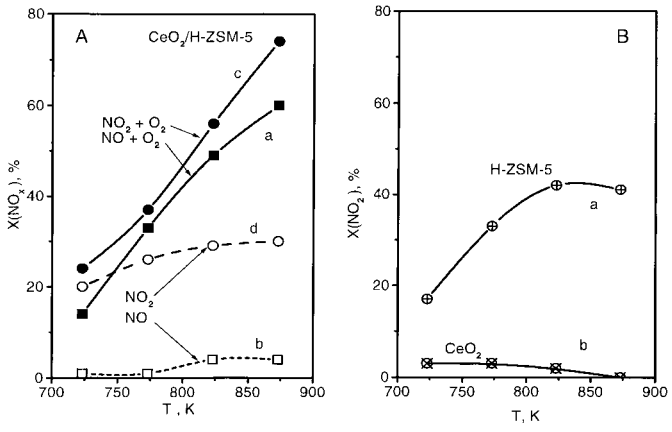

FIG. 5. Selective catalytic reduction of NO_2 by methane over CeO_2/H-ZSM-5 catalysts: 1000 ppm NO_2 (or NO); 1000 ppm CH_4; and 2 (or 0)% O_2 in He; catalysts based on ZSM-5(β). (A) Comparison of the reactivity of the CeO_2/H-ZSM-5 precipitate catalyst toward NO_2 and NO in the presence or absence of 2 vol% O_2. Curves: (a) NO, with 2% O_2 (cf. Fig. 3A); (b) NO only; (c) NO_2, with 2% O_2; (d) NO_2 only. (B) Conversion of NO_2 (in the presence of O_2!) over the catalyst components. Curves: (a) H-ZSM-5; GHSV = 10,000 h^{-1}; (b) CeO_2, GHSV = 250,000 h^{-1} (i.e., the GHSV seen by the CeO_2 component in precipitate catalysts under standard conditions). In the case of NO_2, X denotes conversion to N_2.

exceeding that of the SCR runs. The results were compared with the NO reduction activity obtained with physical mixtures of CeO_2 with the corresponding zeolites (Fig. 6). Figure 6A shows that CeO_2 is by far the most active NO oxidation catalyst among the substances studied (the conversions measured with the zeolites, e.g., H-Beta, refer to considerably lower GHSV, cf. Experimental). Even at the higher space velocity used it provides equilibration between

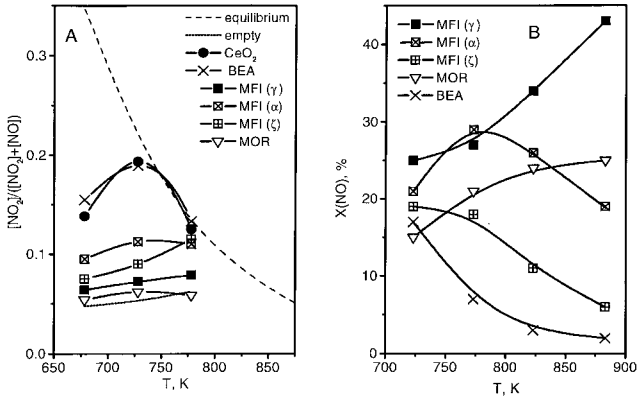

FIG. 6. NO oxidation activity of catalyst components and performance of their mixtures in the selective catalytic reduction of NO with methane. (A) NO oxidation activity of CeO_2 and various zeolites (see inset), compared with equilibrium conversions and empty reactor data; 1000 ppm NO; 2% O_2 in He; GHSV = 55,000 h^{-1} for zeolites, ≈700,000 h^{-1} for CeO_2 (cf. Experimental). (B) NO conversions in the SCR with methane over physical mixtures of CeO_2 with zeolites, the NO oxidation activity of which is reported in panel A. GHSV, 10,000 h^{-1}; 1000 ppm NO; 1000 ppm CH_4; and 2% O_2 in He.

NO and NO_2 already at 723 K. For reasons not understood so far, the NO oxidation activity of the zeolites studied is very divergent and clearly not correlated with either the Si/Al ratio or the zeolite type.

Moreover, comparison of the NO oxidation activity of the various zeolites with the SCR activity of CeO_2-containing mixtures with them reveals no correlation between these two catalytic functions (Figs. 6A, 6B). Conversely, the performance of the CeO_2/H-Beta mixtures in NO reduction is disappointing although H-Beta is a good NO oxidation catalyst while H-ZSM-5 and H-MOR samples, which possess very low NO oxidation activity, provide much better SCR catalysts. This seems even to indicate that zeolite NO oxidation activity, which is known to be necessary for the SCR reaction to proceed over acidic zeolites (22) (i.e., in the *absence* of CeO_2), may even interfere with the particular reaction mechanism that provides the excess activity induced by the presence of CeO_2. It is apparent from these results that the NO oxidation function has to be assigned to the extrazeolite CeO_2 in the composite system.

In our catalytic experiments it was found that the CeO_2 surface accumulates NO_x at temperatures between 570 and 670 K, probably in the nitrate form, which leads to imperfect N balances in this temperature range. NO_x adsorbed on CeO_2 by treatment with 1000 ppm NO, 10% O_2 in He at 673 K, with subsequent cooling in the same gas flow, desorbed in a subsequent TPD experiment (10 K/min) in two peaks at ≈673 (as NO_2) and ≈773 K (NO).

Methane Activation and Transfer Step between Sites

The assignment of the methane activation sites is less straightforward since the activated form will easily couple with NO_2 (or be produced by interaction with NO_2) and rapidly undergo consecutive reactions leading to N_2 and carbon oxides. The position of the transfer step between redox and acidic sites in the reaction sequence (prior to or after methane activation) is also of relevance for the identification of the methane activation site.

Figure 5B shows NO_2 conversions in the reaction with methane over H-ZSM-5 (curve a) and CeO_2 (curve b). These data should be compared with curve c in Fig. 5A, which reports the NO_2 conversion over the complete catalyst under the same conditions. It is obvious that CeO_2 alone is unable to reduce even NO_2 to N_2 with methane (Fig. 5B, curve b). H-ZSM-5 provides measurable conversions, which are, however, significantly exceeded by the conversions over the complete catalyst particularly at high temperatures (Fig. 5A, curve c). The latter would not be expected if the equilibration of NO and NO_2 were the only function of CeO_2 in the SCR reaction sequence, with the remaining steps proceeding on zeolite sites. At temperatures of 823–873 K, the equilibrium NO_2 concentration formed from our standard feed mixture is in the range of only 75–50 ppm. This is rapidly established in the presence of

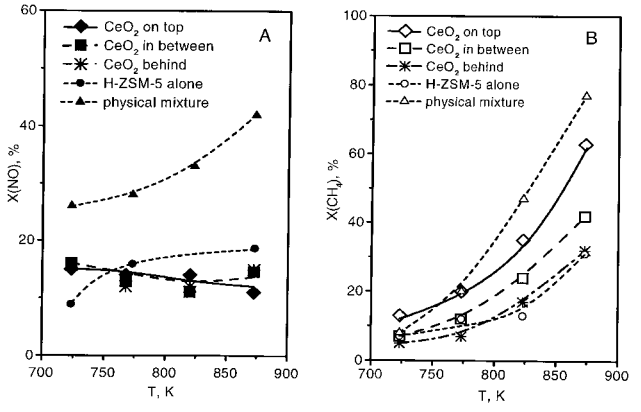

FIG. 7. Selective catalytic reduction of NO with methane over CeO_2 and H-ZSM-5(γ) arranged in layers: 150 mg of CeO_2 preceding/following the zeolite (900 mg), or placed in intermediate position (relative to gas flow), comparison with activity of fully mixed components and of H-ZSM-5. GHSV, 10,000 h^{-1}; 1000 ppm NO; 1000 ppm CH_4; and 2% O_2 in He.

CeO_2. Over the pure H-ZSM-5, the NO_2 concentration should remain significantly higher along the catalyst bed; hence, larger N_2 formation should be found in the absence of CeO_2. Since the opposite is true, the interaction between methane and NO_x obviously starts on the CeO_2 surface.

A similar conclusion was derived from an experiment in which CeO_2 and H-ZSM-5 (γ) were arranged in consecutive layers. These components provide NO conversions of ≈40% when completely mixed (Fig. 7, curves "physical mixture," X(NO) cited from Fig. 6B). Figure 7 reports NO and methane conversions for arrangements with CeO_2 on top of, in the middle of, or behind the zeolite bed and compares them with the results of the physical mixture and the pure H-ZSM-5. If the function of CeO_2 was just to provide NO_2 for a consecutive reaction over zeolite sites, the NO conversion should decrease significantly as the ceria is moved behind the catalyst bed. Instead, the NO conversion remains constant and low (panel A) while the methane conversions decrease (panel B). The latter proves that the NO_2 formed over the CeO_2 is, indeed, transported along the zeolite bed, but at the low concentrations possible above 750 K it obviously boosts only the methane total oxidation. Hence, the contact between hydrocarbon and NO_2 (nitrate) required for NO_x reduction to proceed occurs on the CeO_2 surface. In addition, Fig. 7 allows us to conclude that the lifetime of the species that mediates the bifunctional interaction between CeO_2 and zeolite sites is short: only real mixtures or precipitates, where CeO_2 and zeolite are in close contact, exhibit the synergetic interaction between these components.

This short-range transfer step may be directed from zeolite to ceria or *vice versa*. In the first case, the short-lived intermediate would have to be an activated methane, i.e., a methyl radical. Although the ability of H-ZSM-5 to form methyl radicals from methane at elevated temperatures cannot be ruled out, it certainly does not play a significant role in the reaction mechanism under discussion. Since only a small part of the zeolite crystal is near the external surface, i.e., near CeO_2, most of the methyl radicals formed in the bulk of the zeolite particles would have to react with the NO_2 provided by the ceria in a radical scheme, i.e., to carbon oxides and NO. Such a mechanism could not explain any significant selectivity of the catalyst for the NO reduction path.

The other transfer direction (CeO_2 → zeolite) implies that the activation of methane occurs also on the CeO_2 surface. This may be achieved with or without the assistance of the adsorbed NO_2 (or nitrate) species. In the TPD experiment after accumulation of NO_x on the CeO_2 surface from a NO/O_2 stream, NO was desorbed peaking at 773 K (*vide infra*), presumably as a result of a thermal reduction of nitrate species. The presence of NO and O_2 may increase the stability of this species, which might be, therefore, a candidate for the $NO_{2,ads}$ or nitrate reaction intermediate mentioned. There is evidence in the literature that CeO_2 has a low tendency to release methyl radicals into the gas phase (28). This does not necessarily mean that it is not able to form these radicals, but they may undergo consecutive oxidation steps on the surface. In the presence of chemisorbed NO_2 (or nitrate) the methyl radicals might be trapped to form nitromethane, which is detached from the surface. Alternatively, nitro- or nitrosomethane may be formed in a NO_2-assisted methane activation step. In this model, the fate of these intermediates depends on their next surface contact: if this surface is CeO_2 (as in the pure oxide) or a zeolite without suitable active sites (Na-ZSM-5), they undergo radical reactions resulting in carbon oxides and NO. When, however, the CeO_2 crystal is adjacent to (or supported on) an acidic zeolite crystal a significant amount of the reactive intermediates has the chance to escape into the zeolite where they are further activated by Brønsted sites and undergo transformations to nitrogen and carbon oxides, which have been discussed in the literature (29–32).

This reaction mechanism may be summarized as shown in Scheme 1. While we do not claim that this scheme reflects all surface processes in detail, it illustrates that over CeO_2/

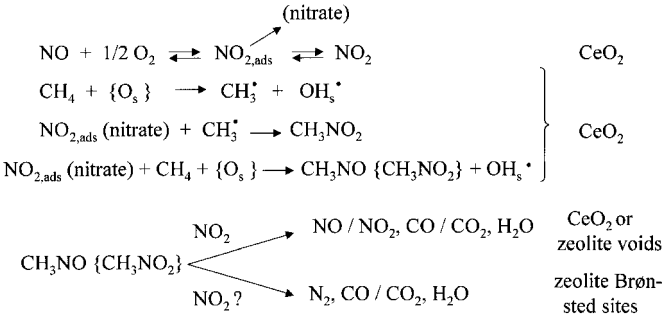

SCHEME 1

H-ZSM-5 catalysts the bifunctional cooperation proceeds via a reaction sequence that is very much different from other mechanisms discussed in the literature so far, where mere supply of NO_2 is often the only function assigned to one of the catalyst components (14, 23–26, 33). A bifunctional mechanism, which includes a short-lived intermediate species mediating the interaction between separate redox and acidic sites has been reported recently for HC-SCR (reductant propane) over Pt/Al_2O_3 (34) but the details of the reaction path derived differ from our conclusions. It should be noted that bifunctionality mediated via gas-phase NO_2 is more favorable from a technological point of view than the scheme presented above since the latter prevents any technology involving reductant supply behind the oxidizing catalyst component (33). Moreover, it will be shown in a subsequent paper that the mechanism detected in our work is very prone to reversible poisoning by water and to irreversible deactivation by zeolite dealumination (35). In summary, the present work confirms that bifunctionality may be realized by different mechanisms in catalysts for HC-SCR. Which type of mechanism is operative may be elucidated by experiments in which the component that supplies NO_2 is separated from the remaining catalyst (cf. Fig. 7).

CONCLUSIONS

NO may be selectively reduced by methane over catalysts consisting of CeO_2 admixed to or precipitated onto H-zeolites, in particular H-ZSM-5. The catalytic functions of this system have been studied by reaction experiments and FTIR spectroscopy. The reaction proceeds via a bifunctional mechanism, in which redox sites on the CeO_2 surface cooperate with protonic sites of the zeolite; however, it was proved that the bifunctional interaction is not mediated by NO_2. It is suggested that a short-lived intermediate (nitro- or nitrosomethane) is formed from adsorbed NO_2 or nitrate and methane on the CeO_2 surface, which has to activate both NO and methane. The intermediate is detached from the CeO_2 sites and transformed to nitrogen and carbon oxides over Brønsted sites of the adjacent zeolite. In the voids of inactive zeolites (e.g., Na forms) or upon further contact with CeO_2, the intermediate undergoes unselective radical chemistry resulting in carbon oxides and NO. This mechanism is basically different from other bifunctional mechanisms for HC-SCR discussed in the literature so far.

ACKNOWLEDGMENTS

Our work was financially supported by the Deutsche Forschungsgemeinschaft, which we gratefully acknowledge. Thanks are due to Dr. E. Brunner (Leipzig University) and Dr. I. Wolf (Ruhr University Bochum) for performing ^1H and ^{27}Al NMR measurements, respectively, and to Prof. N. W. Cant (Macquarie University, Australia) for inspiring discussions.

REFERENCES

1. Shelef, M., *Chem. Rev.* **95**, 209 (1995).
2. Armor, J. N., *Catal. Today* **26**, 147 (1995).
3. Burch, R., and Millington, P. J., *Catal. Today* **26**, 185 (1995).
4. Misono, M., and Kondo, K., *Chem. Lett.* 1001 (1991).
5. Nishizaka, Y., and Misono, M., *Chem. Lett.* 1296 (1993).
6. Grünert, W., Papp, H., Rottländer, C., and Baerns, M., *Chem. Tech. (Leipzig)* **47**, 205 (1995).
7. Käßner, P., Grünert, W., and Papp, H., *Chem. Tech. (Leipzig)* **48**, 77 (1996).
8. Liese, T., Rutenbeck, D., and Grünert, W., "Proceedings, 12th International Zeolite Conference, Baltimore, MD, July 5–10, 1998" (M. M. J. Treacy, B. K. Marcus, M. E. Bisher, and J. B. Higgins, Eds.), MRS Conference Proceedings, Vol. IV, pp. 2975–2802. Mater. Res. Soc., Warrendale, PA, 1998.
9. Jansen, J., van der Gaag, F. J., and van Bekkum, H., *Zeolites* **4**, 369 (1984).
10. Liese, T., and Grünert, W., unpublished results.
11. Liese, T., Ph.D. thesis, Ruhr-Universität, Bochum, 1999.
12. Kikuchi, E., Ogura, M., Aratani, N., Sugiura, Y., Hiramoto, S., and Yogo, K., *Catal. Today* **27**, 35 (1996).
13. Li, Y., and Armor, J. N., *Appl. Catal. B* **2**, 239 (1993).
14. Freude, D., Hunger, M., and Pfeiffer, H., *Z. Phys. Chem. N. F.* **152**, 171 (1987).
15. Yokoyama, C., and Misono, M., *Catal. Lett.* **29**, 1 (1994).
16. Jacobs, P. A., and van Ballmoos, R., *J. Phys. Chem.* **86**, 3050 (1982).
17. Löffler, E., Lohse, U., Peuker, C., Oehlmann, G., Kustov, L. M., Zholobenko, V. L., and Kazansky, V. B., *Zeolites* **10**, 266 (1990).
18. Löffler, E., Ph.D. thesis, Universität Bremen, 1997.
19. Lago, R. M., Haag, W. O., Mikovsky, R. J., Holson, D., Hellring, S. D., Schmitt, K. D., and Kerr, G. T., "Proceedings 7th International Zeolite Confernce" (Y. Murakami, A. Ijima, and J. W. Ward, Eds.), p. 677. Kodansha, Tokyo, 1986.
20. Haag, W. O., *Stud. Surf. Sci. Catal.* **84**, 1375 (1995).
21. Zholobenko, V. L., Kustov, L. M., Kazansky, V. B., Löffler, E., Lohse, U., and Oehlmann, G., *Zeolites* **11**, 132 (1991)
22. Hamada, H., Kintaichi, Y., Sasaki, M., Ito, T., and Tabata, *Appl. Catal.* **70**, L15 (1991).
23. Kikuchi, E., and Yogo, K., *Catal. Today* **22**, 73 (1994).
24. Yokoyama, C., and Misono, M., *J. Catal.* **150**, 9 (1994).
25. Li, Z., and Flytzani-Stephanopoulos, M., *Appl. Catal. A* **165**, 15 (1997).
26. Nishizaka, Y., and Misono, M., *Chem. Lett.* 2237 (1994).
27. Bethke, K. A., Li, C., Kung, M. C., Yang, B., and Kung, H. H., *Catal. Lett.* **31**, 287 (1995).
28. Tong, Y., and Lunsford, J. H., *J. Am. Chem. Soc.* **113**, 4741 (1991).
29. Hayes, N. W., Joyner, R. W., and Shpiro, E. S., *Appl. Catal. B* **8**, 343 (1996).
30. Cowan, A. D., Cant, N. W., Haynes, B. H., and Nelson, P. F., *J. Catal.* **176**, 329 (1998).
31. Lombardo, E. A., Sill, G. A., d'Itri, J. L., and Hall, W. K., *J. Catal.* **173**, 440 (1998).
32. Cant, N. W., Cowan, A. D., Liu, I. O. Y., and Satsuma, A., *Catal. Today* **54**, 473 (1999).
33. Iwamoto, M., Zengyo, T., and Hernandez, A. M., *Res. Chem. Intermed.* **24**, 115 (1998).
34. Inaba, M., Kintaichi, Y., and Hamada, H., *Catal. Lett.* **36**, 223 (1996).
35. Liese, T., Sowade, T., and Grünert, W., to be published.